

On the Dynamics of Bounding and Extensions Towards the Half-Bound and the Gallop Gaits

Ioannis Poulakakis, James Andrew Smith and Martin Buehler
poulakas|jasmith|buehler@cim.mcgill.ca

Ambulatory Robotics Laboratory, <http://www.mcgill.cim.ca/~arlweb>
Centre for Intelligent Machines, McGill University, Montreal, CANADA

Abstract

This paper examines how simple control laws stabilize complex running behaviors such as bounding. First, we reveal and discuss the unexpectedly different local and global forward speed versus touchdown angle relationships in the self-stabilized SLIP model. Then we show that, surprisingly, even for a much more complex, energy conserving quadruped model, many cyclic bounding motions exist, which can be locally, open loop stable! The success of simple bounding controllers motivated the application of similar controllers for asymmetric gaits and resulted in the first experimental implementations of the half-bound and the rotary gallop on our Scout II quadruped.

1. Introduction

Many mobile robotic applications might benefit from the improved mobility and versatility of legs. Twenty years ago, Raibert set the stage with his groundbreaking work on dynamically stable legged robots by introducing a simple and highly effective three-part controller for stabilizing running on his one-, two-, and four-legged robots [13]. Other research showed that even simpler control laws, which do not require task-level or torso-state feedback, can stabilize running as well [1]. Indeed, previous work on the quadruped robot Scout II (Fig. 1) showed that *open loop* control laws that simply position the legs at a desired touchdown angle, result in stable running at speeds over 1 m/s [17].

Motivated by experiments on cockroaches, Kubow and Full studied the role of the mechanical system in control, by developing a simple two-dimensional dynamic model of a hexapedal runner (death-head cockroach, *Blaberus discoidalis*), [8]. The model included no equivalent of nervous feedback and it was found to be inherently stable. This work first revealed the significance of *mechanical* feedback in simplifying neural control by demonstrating that stability could result from leg moment arm changes alone.

Full and Koditschek set a foundation for a systematic study of legged locomotion by introducing the concepts of *templates* and *anchors* [3]. To study the basic properties of sagittal plane running, the *Spring Loaded Inverted Pendulum (SLIP)* template has been proposed, which describes running in

animals that differ in skeletal type, leg number and posture [3]. Recently, Seyfarth et. al., [16], and Chigliazza et al., [2], found that for certain leg touchdown angles, the SLIP becomes self-stabilized if the leg stiffness is properly adjusted and a minimum running speed is exceeded. As speed increases, the system becomes less sensitive to perturbations.



Figure 1. Scout II: A simple four-legged robot.

Motivated by these results, we first describe some interesting aspects of the relationship between forward speed and leg touchdown angles in the SLIP self-stabilized regime. Next we attempt to provide an explanation for simple control laws being adequate in stabilizing complex tasks such as bounding, based on a simple sagittal “template” model. Passively generated cyclic motions are identified based on a return map and a regime where the system is self-stabilized is also found. Furthermore, motivated by the success of simple control laws to generating bounding running, we extended the bounding controllers, proposed in [17] to allow for asymmetric three-beat and four-beat gaits.

Following in the footsteps of Raibert, much of the work on quadrupedal locomotion in McGill’s Ambulatory Robotics Laboratory has been devoted to the symmetric bounding gait [17]. The half-bound, as illustrated in [4] and [7] expands our robots’ gait repertoire, and introduces an asymmetry to the bound, in the form of the leading and trailing front legs, while the back legs’ motion remains symmetric about the sagittal plane. The rotary gallop is another new addition with leading and trailing legs in both the front and rear of the robot. The four-beat sequence of

the touchdowns of the robot's feet are similar to those found in [6] and in [15]. Our first experimental implementations, reported here, of the half-bound and the rotary gallop to the Scout II platform leads to a possible study of three-dimensional motion outside of the sagittal plane. To the authors' best knowledge this is the first implementation of both the half-bound and the gallop (rotary or otherwise) in a robot.

2. Bounding Experiments with Scout II

Scout II (Fig.1) has been designed for power-autonomous operation. One of the most important features is that it uses a *single* actuator per leg – the hip joint provides leg rotation in the sagittal plane. Thus, each leg has two degrees of freedom (DOF): the actuated revolute hip DOF, and the passive linear compliant leg DOF.

In the full bound the essential components of the motion take place in the sagittal plane. In [17] we propose a controller which results in fast and robust bounding running without full-state feedback. The controller is based on two individual, independent front and back virtual leg controllers. The front and back virtual legs each detect two leg states - stance and flight. During flight, the controller serves the flight leg to a desired, fixed, touchdown hip angle. During stance the leg is swept back with a constant commanded torque until a sweep limit is reached. Note that the actual applied torque during stance is determined primarily by the motor's torque-speed limits, until the sweep limit is reached, [17]. This controller results in robust bounding with forward speeds up to 1.3 m/s. The sequence of the phases of the resulting bounding gait is given in Fig. 2.

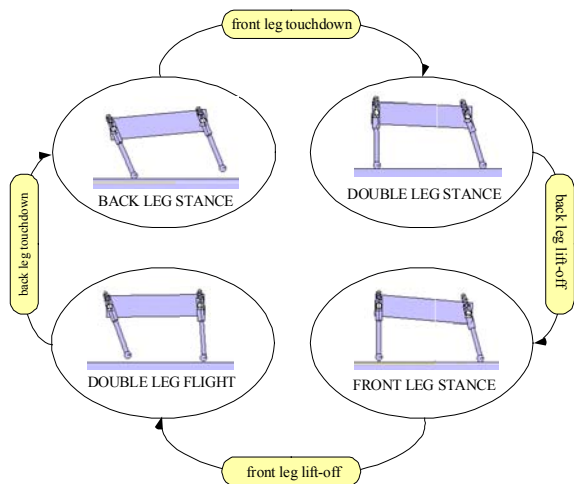


Figure 2. Bounding phases and events.

Scout II is an under-actuated, highly nonlinear, intermittent dynamic system. The limited ability in applying hip torques due to actuator and friction

constraints and due to the existence of unilateral ground forces further increases the complexity. Furthermore, as Full and Koditschek state in [3], “locomotion results from complex high-dimensional, dynamically coupled interaction between an organism and its environment”. Thus, the task itself is complex too, and cannot be specified via reference trajectories. Despite this complexity, simple control laws, like the one described above and in [17], can stabilize periodic motions, resulting in robust and fast running *without* requiring any task level feedback like forward velocity. Moreover, they do *not* require body state feedback.

It is therefore natural to ask why such a complex system can accomplish such a complex task without task level feedback control action. As outlined in this paper and in more detail in [11] and [12], a possible answer is that Scout II's unactuated, conservative dynamics *already* exhibit stable bounding cycles, and hence a simple controller is all that is needed for keeping the robot bounding.

3. Self-stabilization in the SLIP

Kubow and Full discovered that the horizontal dynamics of sprawled postured animals can be stable without the need of feedback control laws [8]. This celebrated result suggests the significance of the mechanical system in self-stabilization. Seyfarth et. al. [16] and Chigliazza et. al. [2], independently extended those results to sagittal plane templates, where, based on return map studies, a proof of the passive stabilization of the SLIP (Fig. 3) has been given.

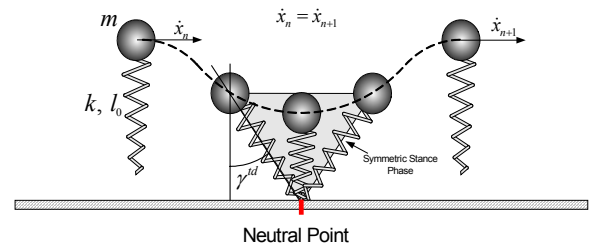


Figure 3. Spring Loaded Inverted Pendulum (SLIP): Neutral point and symmetric stance phase.

It is important to mention here that the mechanism that results in that self-stabilizing property is not yet fully understood, at least in a way that could immediately be applicable to improve existing control algorithms. It is known that for a set of initial conditions (forward speed and apex height), there exists a touchdown angle at which the system maintains its initial forward speed. These conditions correspond to starting the system at a point that lies on the periodic cycle and are referred to as the *neutral point*, see Fig. 3. As Raibert noticed, [13], if the fixed

point is perturbed by changing the touchdown angle, e.g. by decreasing it, then the system will accelerate in the first cycle. Thus, at the second step the forward speed will be greater than that at the first, and if the touchdown angle is kept constant the system will accelerate in the subsequent steps and finally fail due to toe stubbing (the kinetic energy increases at the expense of the potential energy resulting in lower apex heights).

However, when the parameters are within the self-stabilization regime, the system does not fall! It adjusts its lift-off angle (the touchdown angle is kept constant) until it converges to a periodic motion at higher forward speed where the stance phase is symmetric. Therefore, not only the touchdown but also the lift-off angle affects the energy distribution between the forward and vertical motions. This fact is not captured in Raibert's linear steady-state argument, [13], based on which one would be unable to predict the self-stabilization behavior of the system. Note, though, that the lift-off angle affects the motion in a nonlinear way that totally depends on the dynamics of the system. Moreover, this angle cannot be controlled like the touchdown angle; it is an output and not an input.

A question we address next is what is the relationship between the forward speed at which the system converges, called the *speed at convergence*, and the touchdown angle. To this end, simulation runs have been performed in which the initial apex height and initial forward velocity are fixed and therefore, the energy level is fixed, while the touchdown angle changes in a range where cyclic motion is achieved. For a given energy level, this results in a curve relating the speed at convergence to the touchdown angle. Subsequently, the apex height is kept constant, while the initial forward velocity varies between 5 and 7 m/s. This results in a family of constant energy curves, which are plotted in Fig. 4.

It is interesting to see in Fig. 4 that in the self-stabilizing regime of the SLIP, an increase in the touchdown angle *at constant energy* results in a lower forward speed at convergence. This means that higher forward speeds can be accommodated by smaller touchdown angles, which, at first glance, is not in agreement with the *global* behavior that higher speeds require bigger (flatter) touchdown angles. This global behavior is also evident in Fig. 4, where it can be seen that forward speeds about, for example, 5 m/s require touchdown angles in the range 21° - 23.75° , while higher speeds such as those about 7 m/s require larger touchdown angles, which lie in the range 25.75° - 30° .

The fact that *globally* fixed points at higher speeds require greater (flatter) touchdown angles was reported by Raibert, [13], and it was used to control the forward speed of his robots based on a feedback control law. However, Fig. 4 suggests that in the

absence of control, i.e. when the system is open loop, and *for a constant energy level*, a reduction in the touchdown angle results in an increase of the speed at convergence. Therefore, one must be careful enough not to transfer results from the case of systems actively stabilized to the case of passive systems, because otherwise opposite outcomes from those expected may result. It must be mentioned though that there might exist combinations of parameters (initial speed, total energy and touchdown angle) in which the local behavior is the opposite of that presented in Fig. 4. This fact illustrates that direct application of the above results in controllers is far from trivial, [11].

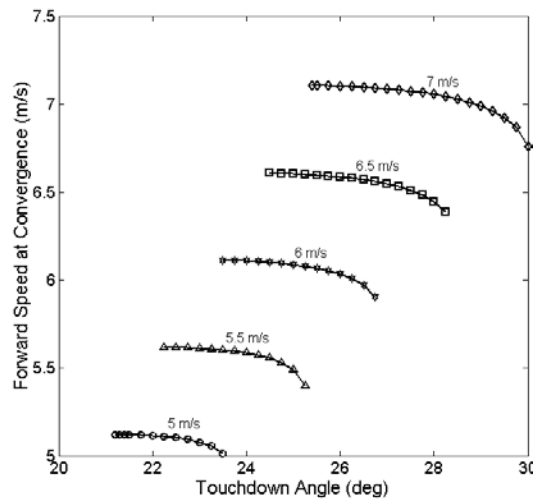


Figure 4. Forward speed at convergence versus touchdown angle at fixed points obtained for initial forward speeds from 5 to 7 m/s and for an apex height equal to 1m.

4. Modeling the Bounding Gait

Motivated by the recent results discussed above, we studied the passive dynamics of Scout II based on the template model shown in Fig. 5. First, we determine the conditions for steady state cyclic motion.

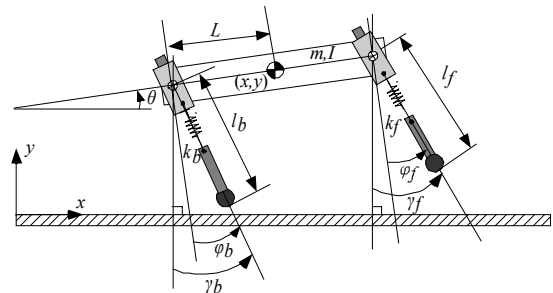


Figure 5. A template for studying sagittal plane running.

To simplify the equations of motion for Scout II, we assume massless legs. Also, a toe in contact with the ground is treated as a frictionless pin joint. In each phase, the equations of motion are

$$\frac{d}{dt} \begin{bmatrix} \mathbf{q} \\ \dot{\mathbf{q}} \end{bmatrix} = \begin{bmatrix} \dot{\mathbf{q}} \\ -\mathbf{M}^{-1}(\mathbf{V} + \mathbf{F}_{el} + \mathbf{G}) \end{bmatrix}, \quad (1)$$

where $\mathbf{q} = [x \ y \ \theta]^T$, see Fig. 5, \mathbf{M} is the mass matrix and \mathbf{V} , \mathbf{F}_{el} and \mathbf{G} are the vectors of the velocity dependent forces, the elastic and the gravitational forces, respectively. The transition conditions for touchdown and lift-off events are

$$y \pm L \sin \theta \leq l_0 \cos \gamma_i^{td}, \quad (2a)$$

$$l_i^{lo} = l_0, \quad (2b)$$

where $i = b, f$ for the back (- in (2a)) and front (+ in (2a)) virtual leg respectively.

The bounding cycle presented in Fig. 2 can be modeled by defining a return map. To do so the apex height in the double leg flight phase is used as a reference point. The states at the n^{th} apex height constitute the initial conditions for the cycle, based on which we integrate successively the dynamic equations of all the phases. This process yields the state vector at the $(n+1)^{\text{th}}$ apex height, which is the value of the return map calculated at the n^{th} apex height. We seek conditions for which the resulting state vector at the new apex height is identical to the initial state vector. These “re-entry” conditions result in repetitive, cyclic motion. In other words we search for fixed points of the return map $\mathbf{P} : \mathbb{R}^4 \times \mathbb{R}^2 \rightarrow \mathbb{R}^4$,

$$\mathbf{x}_{n+1} = \mathbf{P}(\mathbf{x}_n, \mathbf{u}_n), \quad (3)$$

with $\mathbf{x} = [y \ \theta \ \dot{x} \ \dot{\theta}]^T$, $\mathbf{u} = [\gamma_b^{td} \ \gamma_f^{td}]^T$. Note that the touchdown angles are inputs available for control.

To find an argument \mathbf{x} in (3) that maps onto itself, the following equation is solved

$$\mathbf{x} - \mathbf{P}(\mathbf{x}) = \mathbf{0}, \quad (4)$$

for all (experimentally) reasonable values of touchdown angles. The search space is 4-dimensional with two free parameters, since for different values of touchdown angles, different solutions may be obtained. The search is conducted numerically using the Newton-Raphson method. An initial guess, $\mathbf{x}_n^{(0)}$, for the fixed point is updated via

$$\mathbf{x}_n^{(k+1)} = \mathbf{x}_n^{(k)} + \left(\mathbf{I} - \nabla \mathbf{P}(\mathbf{x}_n^{(k)}) \right)^{-1} \left[\mathbf{P}(\mathbf{x}_n^{(k)}) - \mathbf{x}_n^{(k)} \right], \quad (5)$$

where n corresponds to the n^{th} apex height and k corresponds to the number of iterations. Evaluation of (5) until convergence (the error between $\mathbf{x}_n^{(k)}$ and $\mathbf{x}_n^{(k+1)}$ is smaller than $1e-6$) yields the solution for the fixed point. To calculate the value of \mathbf{P} at $\mathbf{x}_n^{(k)}$, we numerically integrate the equations of motion for each phase during a complete cycle using the adaptive step Dormand-Price method with $1e-6$ and

$1e-7$ relative and absolute tolerances, respectively.

Implementation of the above method resulted in a large number of fixed points of the return map \mathbf{P} , for different initial guesses and different touchdown angles. All these fixed points exhibited some very interesting and useful properties concerning the symmetry of the bounding motion. For example, the pitch angle θ was found to be always zero (the body is horizontal) at the apex height. More importantly, for each cycle, the touchdown angle of the front leg is equal to the negative of the lift-off angle of the back leg while the touchdown angle of the back leg is equal to the negative of the lift-off angle of the front leg i.e.

$$\gamma_f^{td} = -\gamma_b^{lo}, \quad \gamma_b^{td} = -\gamma_f^{lo}, \quad (6)$$

This last property resembles the case of the SLIP model, in which a necessary and sufficient condition for fixed points is the symmetric stance phase, i.e. the lift-off angle is equal to the negative of the touchdown angle, [2]. These symmetry properties hold for all the fixed points found randomly using the method described above, [11].

It is desired to find fixed points at specific forward speeds and apex heights. Therefore, the search scheme described above is modified so that the forward speed and apex height become its input parameters, specified according to running requirements, while the touchdown angles are now considered to be “states” of the search procedure, i.e. variables to be determined from it, see [11] [12]. By doing so, the *search space* states and the vector of the parameters (“inputs” to the search scheme) are respectively

$$\mathbf{x}^* = [\theta \ \dot{\theta} \ \gamma_b^{td} \ \gamma_f^{td}]^T, \quad \mathbf{u}^* = [y \ \dot{x}]^T. \quad (7)$$

From Fig. 6 it can be seen that there is a continuum of fixed points, which follows an “eye” pattern, accompanied by two external branches. Those fixed points correspond to 1 m/s forward speed, 0.35 m apex height and varying pitch rate. The existence of the external branch implies that there is a range of pitch rates where two *different* fixed points exist for the same forward speed, apex height and pitch rate. This is quite surprising since the same total energy and the same distribution of that energy among the three modes of the motion -forward, vertical and pitch- results in two different motions depending on the touchdown angles. The fixed points that lie on the internal branch of Fig. 6 correspond to a bounding motion where the front leg is brought in front of the torso, while the fixed points that lie on the external branch correspond to a motion where the front leg is brought towards the torso’s Center of Mass (COM).

Repeating the numerical search for higher forward speeds showed that the “eye” pattern shifts to higher values of the touchdown angles, i.e. larger touchdown

angles are required to maintain higher speeds [12]. This fact also agrees with Raibert's findings [13] and with the global behavior shown in Fig. 4. It is useful to note that the region close to the vertical axis corresponds to pronking-like motions. Indeed, recall that, at the apex height $\theta = 0$ always. As the vertical axis of Fig. 6 ($\dot{\theta} = 0$) is approached, the touchdown angles of the front and back legs tend to become equal. A gait with $\theta = 0$, $\dot{\theta} = 0$ and equal touchdown angles for the front and back legs corresponds to the pronking gait, where the front and back legs strike the ground almost in unison. Therefore, points near the vertical axis correspond to pronking-like motions. Useful conclusions concerning the stability of the bounding and the pronking gaits will be discussed in the next section.

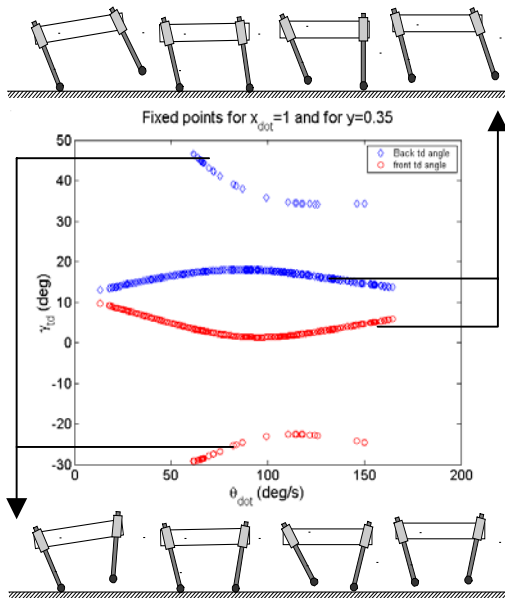


Figure 6. Fixed points for 1m/s forward speed and 0.35 m apex height. Snapshots show the motions corresponding to the fixed points.

5. Local Stability of Passive Bounding

The fact that bounding running cycles can be generated passively in a conservative system as a response to the appropriate initial conditions may have significant implications for control. Indeed, if the system remains close to its passive behavior, then the actuators have less work to do to maintain the motion and energy efficiency, an important issue to any mobile robot, is improved. Most importantly it is also significant to search for operating regimes where the system is passively stable, so that active stabilization will require less control effort and sensing. The local stability of the fixed points found in previous section is now examined. A periodic solution corresponding to a fixed point \bar{x} is stable if

all the eigenvalues of the LTI discrete system matrix

$$\mathbf{A} = \left. \frac{\partial \mathbf{P}(\mathbf{x}, \mathbf{u})}{\partial \mathbf{x}} \right|_{\mathbf{x}=\bar{\mathbf{x}}} \quad (7)$$

have magnitude less than one.

Fig. 7 shows the eigenvalues of matrix \mathbf{A} for forward speed 1 m/s and apex height 0.35 m and varying pitch rate. Note that the same pattern is observed for different forward speeds and apex heights. As it was expected, one of the eigenvalues is always located at one, representing the fact that the system is conservative. Two of the eigenvalues start on the real axis, and as $\dot{\theta}$ increases they move towards each other, they meet on the real axis and finally they move towards the rim of the unit circle. This behavior is an indication for the existence of cyclic coordinates in the Lagrangian, and is currently under investigation. The third eigenvalue starts at a high value and moves towards the unit circle but it never gets into it, for those specific values of forward speed and apex height. Therefore there is no region of parameters where the system is passively stable for speed $\dot{x} = 1 \text{ m/s}$ and apex height $y = 0.35 \text{ m}$.

Root Locus with $\dot{\theta}$ as parameter: $x_{\text{dot}}=1$ and $y=0.35$

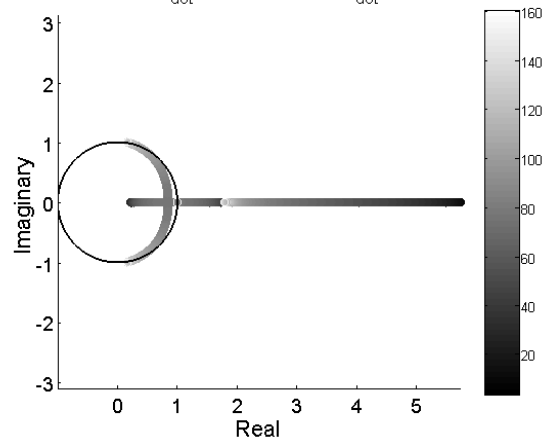


Figure 7. Root locus showing the paths of the four eigenvalues as the pitch rate increases.

To show how the forward speed affects the stability of the motion we present Fig. 8, which shows the magnitude of the larger eigenvalue at different forward speeds. For sufficiently high forward speeds and pitch rates, the larger eigenvalue enters the unit circle while the other two eigenvalues remain well behaved. Therefore, there exists a regime where the system can be passively stable. This is a very important result since it shows that the system can tolerate small perturbations of the nominal conditions *without* any control action taken! This fact could provide a possible explanation to why the Scout II robot can bound, without the need of complex state feedback. It is important to mention that this result is

in agreement with recent research from biomechanics, which shows that when animals run at high speeds, passive dynamic self-stabilization from a feed-forward, tuned mechanical system can reject rapid perturbations and simplify control [3] [8]. Analogous behavior has been discovered by McGeer in his passive bipedal running work [9] and recently in the SLIP template [2] [16].

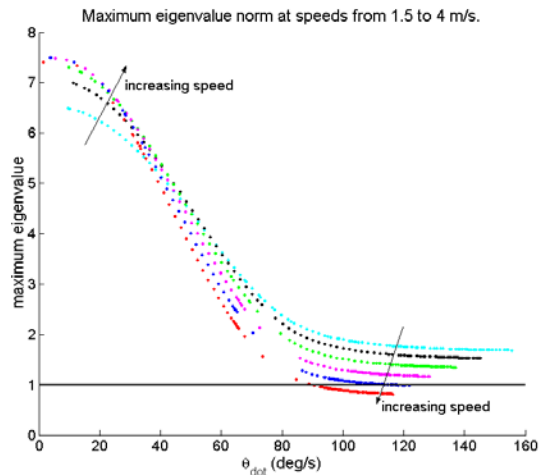


Figure 8. Largest eigenvalue norm at various pitch rates and for forward speeds between 1.5 and 4m/s. The apex height is 0.35 m.

It is important to note that, as depicted in all the above plots (Figs. 7 and 8), the largest eigenvalue obtains its maximum value when the pitch rate $\dot{\theta}$ is small. Recall that the region where $\dot{\theta}$ takes small values corresponds to a pronking-like motion, where both the front and back legs hit and leave the ground in unison. Thus, we can conclude that pronking-like motions (low-pitch rates) are more unstable than bounding, (high pitch rates).

6. Introducing Asymmetry: Half-bound and Rotary Gallop

This section describes extensions of the bounding gait called the half-bound and the rotary gallop. The controllers for both these gaits are generalizations of the original bounding controller, allowing two asymmetric states to be observed in the front lateral leg pair and adding control methods for these new states.

The back lateral leg pair state machine in both controllers is essentially unchanged from the bounding controller; it only has two states, one for when both legs are in stance and one for when both legs are in flight. The front lateral leg pair state machine in both controllers adds two new asymmetric states: the left leg is in flight while the right leg is in

stance, and the left leg is in stance while the right leg is in flight. In the regular bounding state machine these asymmetric states are ignored and state transitions only occur when the lateral leg pair are either both in stance or both in flight; in other words, no new control action occurs until both legs are in the same state. The control action associated with the asymmetric states enforces a phase difference between the two legs during each leg's flight stage, but is otherwise unchanged from the bounding controller as presented in [17].

The following is the description of the control actions taken for the front legs. Leg 1 (front, left side) is the first to touchdown; Leg 3 (front, right side) touches down after Leg 1.

Case 1: Leg 1 (1st to touchdown) and Leg 3 (2nd to touchdown) are both in flight. Leg 1 is actuated to a predetermined touchdown angle (17 degrees from vertical, with respect to the body's local coordinate system). Leg 3 is actuated to a larger touchdown angle (32 degrees) to enforce separate touchdown times.

Case 2: Leg 1 and Leg 3 are both in stance. Both legs are commanded to actuate with a constant torque unless they reach an angle of 0 degrees with respect to the body's vertical, at which point the legs must remain at this angle.

Case 3: Leg 1 is in stance and Leg 3 is in flight. Leg 1 is commanded to move with the same torque as in Case 2 and to the same limit angle. Leg 3 is commanded to position itself at the same angle as it is in Case 1. This case occurs at the beginning of Leg 1's stance phase.

Case 4: Leg 1 is in flight and Leg 3 is in stance. Leg 1 is commanded to reach the predetermined touchdown angle, as outlined in Case 1. Leg 3 is commanded to actuate with a constant torque until it reaches a sweep limit angle of 0 degrees with respect to the body's vertical, as in Case 2.

Application of the half-bound controller results in the motion shown in the sequence of photos in Fig. 9. Although it has been studied in biological systems, see [4] and [7], to the authors' best knowledge this is the first implementation of a half-bound running gait on a robot. Fig. 10 illustrates how the two front legs are actuated to two separate touchdown angles (Leg 1: 17 degrees; Leg 3: 32 degrees) and maintain an out-of-phase relationship during stance, while the back two legs have virtually no angular phase difference at any point during the motion.

Fig. 11 illustrates the states of the two lateral leg pairs throughout the half-bound motion. The graph shows that Leg 1 touches down prior to Leg 3 and also takes off first. Motion stabilizes approximately one second after it begins (at the 132 second mark), with the back legs showing only a minor phase difference. This phase difference is a result of the roll induced during the touchdown of the out-of-phase

front legs. The effect of the half-bound motion on yaw on the Scout II platform is currently under investigation.

The major difference between both the bound and the half-bound controllers and the gallop controller is that a phase difference of 15 degrees (touchdown angles: Leg 4: 17 degrees; Leg 2: 32 degrees) is enforced between the leading and trailing rear legs during the double-flight phase.

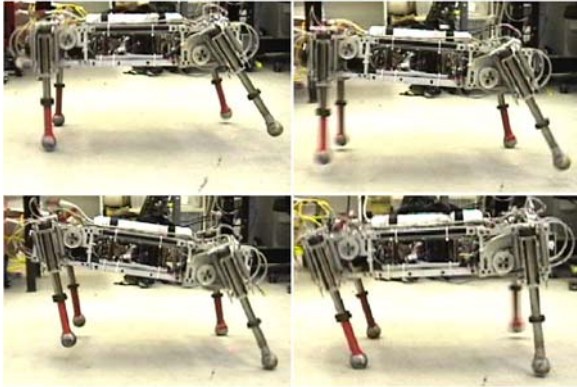


Figure 9. Snapshots of the sequence of the phases during the half bound: back legs (Legs 2 and 4) in stance, front left leg (Leg 1) touchdown, front right leg (Leg 3) touchdown, back legs (Legs 2 and 4) touchdown.

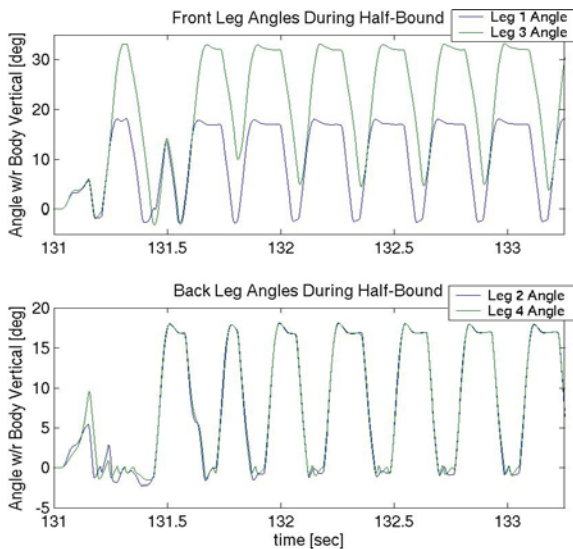


Figure 10. Front and back leg angles in the half-bound.

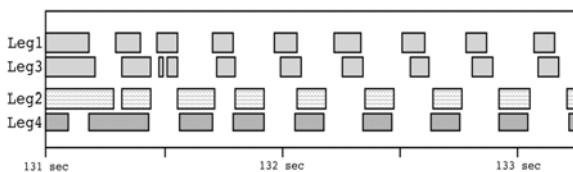


Figure 11. Front (Legs 1 and 3) and back (Legs 2 and 4) leg stance phases in the half-bound: Shaded blocks represent stance periods.

Application of the rotary gallop controller results in the motion shown in the sequence of the plots in Fig. 12. As with the half-bound the rotary gallop has been studied in biological systems [6], [7] and in simulations [5], [15] but to the authors' best knowledge it has never been implemented in a robot. Fig. 13 illustrates how the front and back leg pairs are actuated to out-of-phase touchdown angles (Leg 1: 17 degrees, Leg 3: 32 degrees, Leg 4: 17 degrees, Leg 2: 32 degrees).

Figure 14 illustrates the stance phases for the four legs. It clearly shows the four-beat footfall pattern necessary for the rotary gallop.

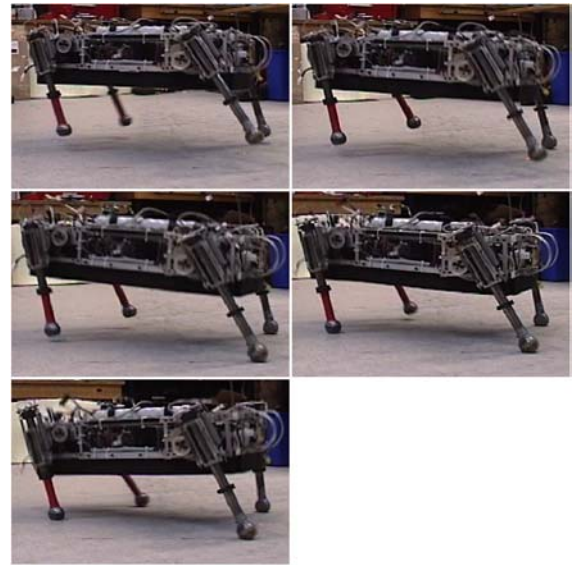


Figure 12. Snapshots of the rotary gallop touchdown sequence: All legs in flight, first front leg (Leg 1) touching down. Second front leg (Leg 3) touching down, first back leg (Leg 4) touching down and second back leg (Leg 2) touching down.

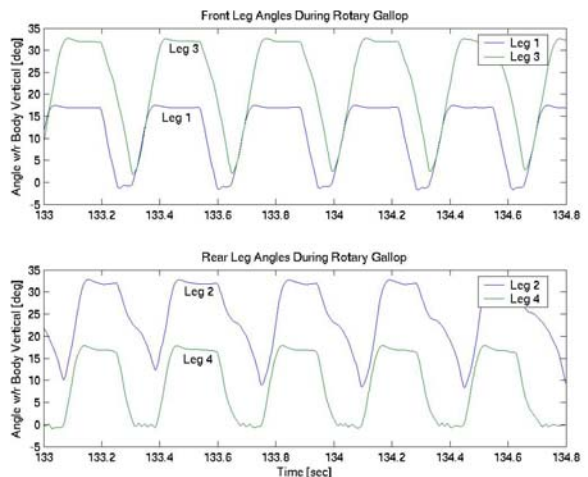


Figure 13. Front and back leg angles in the rotary gallop.

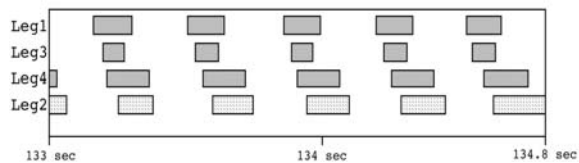


Figure 14. Front (Legs 1 and 3) and back (legs 2 and 4) leg stance phases in the rotary gallop: Shaded blocks represent stance periods.

7. Conclusion

This paper examined the difference between the local and global speed versus touchdown angle relationships in the self-stabilized (monoped) SLIP model. It then showed that a much more complex model for quadruped sagittal plane running can still exhibit similar passively generated bounding cycles with appropriate initial conditions. Most strikingly, there exists a regime where the model stabilizes itself without the need of any control action. This might explain why simple controllers, as reported in [17], are adequate in stabilizing a complex dynamic task like quadruped running. Self-stabilization can facilitate the design of control laws for dynamically stable legged locomotion by designing controllers that expand the domain of attraction of that behavior. These controllers are currently under investigation. Also, these results are in agreement with recent results from biomechanics. Furthermore, preliminary experimental results showing Scout II exhibiting the half-bound and rotary gallop running gaits have been presented. Future work includes the application of the half-bound and rotary gallop gaits to improving maneuverability on the Scout II platform.

Acknowledgments

Support by IRIS III, Canadian Centres of Excellence, and by NSERC is gratefully acknowledged. The work of I. Poulakakis has been supported by a R. Tomlinson Doctoral Fellowship Award and by the Greville Smith McGill Major Scholarship.

References

- [1] Buehler M., "Dynamic Locomotion with One, Four and Six-Legged Robots", in *J. of the Robotics Society of Japan*, 20 (3), pp. 15-20, 2002.
- [2] Chigliazza R. M., Altendorfer R., Holmes P. and Koditschek D. E., "Passively Stable Conservative Locomotion", submitted to *SIAM J. of Applied Dynamical Systems*.
- [3] Full R. J. and Koditschek D., "Templates and Anchors: Neuromechanical Hypotheses of Legged Locomotion on Land", in *J. of Experimental Biology*, 202, pp. 3325-3332, 1999.
- [4] Hackert, R., Witte H. and Fischer M. S., "Interaction between motions of the trunk and the limbs and the angle of attack during synchronous gaits of the pika (*Ochotona rufescens*)", *Int. S. on Adaptive Motion of Animals and Machines*, 2000.
- [5] Herr H. M. and McMahon T. A., "A Galloping Horse Model", in *Int. J. of Robotics Research*, 20, pp. 26-37, 2001.
- [6] Hildebrand M., "Motions of the Running Cheetah and Horse", in *J. of Mammalogy*, Vol. 40, No. 4, Nov. 20, pp. 481-495, 1959.
- [7] Hildebrand M., "Analysis of Asymmetrical Gaits" Milton, in *J. of Mammalogy*, Vol. 58, 31, pp. 131-156, 1977.
- [8] Kubow T. and Full R., "The Role of the Mechanical System in Control: A Hypothesis of Self-stabilization in Hexapedal Runners" in *Phil. Trans. R. Soc. of Lond. B – Biological Sciences* 354 (1385), pp. 854-862, 1999.
- [9] McGeer T., "Passive Bipedal Running", *Technical Report, CSS-IS TR 89-02*, Simon Fraser University, Centre For Systems Science, Burnaby, BC, Canada, 1989.
- [10] Nichol J. G. and Waldron K. J., "Biomimetic Leg Design for Untethered Quadruped Gallop", in *Int. Conf. of Climbing and Walking Robots (CLAWAR)*, 2002.
- [11] Poulakakis I., *On the Passive Dynamics of Quadrupedal Running*, M. Eng. Thesis, McGill University, Montreal, QC, Canada, July 2002.
- [12] Poulakakis I., Papadopoulos E. and Buehler M., "On the Stable Passive Dynamics of Quadrupedal Running", to appear in *IEEE Int. Conf. on Robotics and Automation*, 2003.
- [13] Raibert M. H., *Legged Robots that Balance*, MIT Press, Cambridge MA, 1986.
- [14] Saranli U., Buehler M., and Koditschek D. E., "RHex: A Simple and Highly Mobile Hexapod Robot", in *Int. J. Robotics Research*, Vol. 20, No. 7, pp. 616-631, 2001.
- [15] Schmiechler J. P. and Waldron K. J., "The Mechanics of Quadrupedal Galloping and the Future of Legged Vehicles", in *Int. J. of Robotics Research*, 18 (12): 1224-1234, Dec. 1999.
- [16] Seyfarth A., Geyer H., Guenther M. and Blickhan R., "A Movement Criterion for Running", in *J. of Biomechanics*, Vol. 35, pp. 649-655, 2002.
- [17] Talebi S., Poulakakis I., Papadopoulos E. and Buehler M., "Quadruped Robot Running with a Bounding Gait" in *Experimental Robotics VII*, D. Rus and S. Singh (Eds.), pp. 281-289, Springer-Verlag, 2001.